International Journal of Data Science

ISSN online: 2053-082X - ISSN print: 2053-0811
https://www.inderscience.com/ijds

Texture feature extraction of a landscape design image based on the contour wave transform

Wenya Li

DOI: 10.1504/IJDS.2023.10053352

Article History:

Received:	16 June 2022
Accepted:	24 August 2022
Published online:	09 March 2023

Texture feature extraction of a landscape design image based on the contour wave transform

Wenya Li

School of Fine Arts and Art Design,
Henan Vocational University of Science and Technology,
Zhoukou, 466000, China
Email: liwenya4684@163.com

Abstract: In order to optimise the landscape design, this study takes the contour wave transform as the core research object, deeply explores its filter setting and action mechanism, and applies it to the extraction of image texture features of landscape design. The results show that when the number of degraded distortion trend feature points is only 100, the feature extraction accuracy of the algorithm has almost reached 90% and continues to improve with the increase of the number of feature points, which is always much higher than other algorithms. This shows that the texture feature extraction of the landscape design image based on the contour wave transform has strong robustness. The algorithm has good application effects on the recognition and extraction of target image features and the evaluation and analysis of image quality. When mixing all image distortion types, it can obtain better extraction and evaluation results.

Keywords: contour wave transform; gardens; landscape design; image; texture features; extract.

Reference to this paper should be made as follows: Li, W. (2023) 'Texture feature extraction of a landscape design image based on the contour wave transform', *Int. J. Data Science*, Vol. 8, No. 1, pp.39–51.

Biographical notes: Wenya Li received his Bachelor's degree in Art Design from Northwest University of Agriculture and Forestry Science and Technology in 2011. In 2013, he obtained a Master's degree in Landscape Architecture from Northwest University of Agriculture and Forestry. He is now a Lecturer in the Academy of Fine Arts and Art Design, Henan Vocational University of Science and Technology. Her research fields are art design, landscape architecture planning and design.

1 Introduction

Image is the most intuitive way to describe events. It has a wide range of applications, and the image processing technology has been significantly optimised in this process. Different from the extraction and analysis of general image features, it is difficult to extract landscape design images, especially its texture features (Li and Zhang, 2020). In the process of image texture feature acquisition and transmission, due to the varying

degrees of noise influence of external environmental factors and imaging equipment, the basic features of target image information are often covered or submerged by noise, which hinders image segmentation and feature extraction. El-Hoseny et al. (2019) proposed a contour wave image fusion method based on optimisation, and compared the effects of multi-resolution and multi-scale geometric effects on the fusion quality. An optimised multiscale fusion technique of Nonsubsampled Contourlet Transform (NSCT) based on modified central force optimisation (MCFO) and local contrast enhancement technology is proposed. The first step of the fusion method is to match the histogram of one image with that of another image to allow the two images to have the same dynamic range. Then NSCT is used to decompose the image to be fused into its coefficients. (He et al., 2019) proposed an image fusion method used with the new dictionary, which is called Nonsubsampled Contourlet Transform (NSCT) – Simultaneous Sparse Representation (SSR). Experimental results show that the proposed fusion method NSCT-SSR has better fusion effect and anti-noise ability, and is superior to the existing fusion methods based on sparse representation in multi-scale domain and single-scale image domain. In order to obtain more accurate image feature information, corresponding measures need to be taken to realise image noise reduction and maximise the interference impact caused by noise. Contour wave transform is an effective image expression method, which can effectively extract the image edge information and structure information under different resolutions by virtue of its multi-scale characteristics and translation invariance, and finally realise the multi-scale and multi-directional extraction of image features (Liu et al., 2019). In view of this, this topic will explore the texture feature extraction method of landscape design image based on contour waveform transformation, and realise the accurate extraction of multi-scale and multi-directional image features by using the combination of Laplacian Pyramid (LP) decomposition filter and directional filter bank (DFP). Using multiple Kernel learning (MKL) to accurately predict the image quality, combined with the sub-band energy of contour waves in different directions and the action relationship between different contour details, the original threshold is corrected on this basis, and finally the purpose of denoising is achieved. And its effectiveness is verified by relevant experiments.

2 Image texture feature extraction algorithm based on contour wave transform

2.1 Filter setting and action mechanism of contour wave transform

As an effective two-dimensional image representation method, Contourlet transform (CT) can comprehensively describe all kinds of singularity direction information of the image, including image edge information, image texture features, etc. (Liu et al., 2019; Zhu et al., 2019). The transformation process of CT mainly shows the trend from discrete to continuous. The accurate extraction of image features is completed from multi-scale and multi-directional by means of the coordination of the two filters. That is, Laplacian pyramid (LP) decomposition filter and DFP (Ch et al., 2019). LP plays an important role in the implementation of image multi-scale decomposition, and the structural block diagram of its action mechanism is shown in Figure 1.

Figure 1 Decomposition and reconstruction of LP

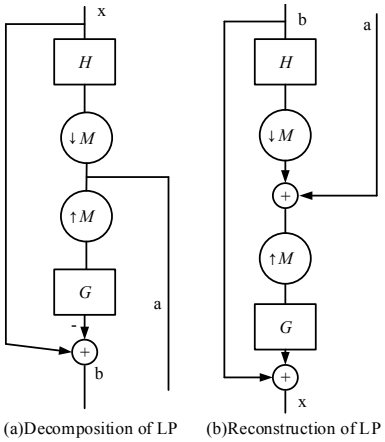

Figure 1(a) shows the decomposition process of LP, where H represents the decomposition filter, M represents the sampling matrix, and G represents the synthesis filter. Firstly, LP needs to generate an original signal x under the joint action of H and M, and set the low-pass part of x as a. Then, carry out up sampling processing and synthesis filtering synthesis processing for a to obtain the prediction signal with the same size as the original image. There is a certain signal difference between x and the prediction image, that is, the high-frequency band communication signal b (Vaidya, 2019). Figure 1(b) shows the reconstruction process of LP. Mainly through the pseudo inverse method, the low-frequency signal of the image is approximated to a, the corresponding up sampling processing and filtering processing are carried out, and then it is superimposed with b to obtain the reconstructed signal x. The reconstruction processing of the signal can eliminate the suppression of the noise signal to a certain extent. When filtering the image signal, the traditional two-dimensional separable filter bank can only make sparse expression in the horizontal, vertical and diagonal directions, which is difficult to effectively process the target image with rich directional features. DFP can effectively improve and solve this problem. The main feature of DFP is that it can accurately divide and extract the image edge contour, and organically combine the fan filter with the rotation sampling matrix, which can significantly simplify the decomposition rules of the image signal on the basis of avoiding modulating the input signal, and finally achieve the goal of directional segmentation (Subhedar and Mankar, 2019). In DFP, it mainly includes two components: dual channel quincunx filter bank and signal clipping. The former can divide the image signal spectrum into horizontal and vertical directions, and the conditions for complete reconstruction are shown in formula (1).

$$\begin{cases} H_0(\omega)G_0(\omega)+H_1(\omega)G_1(\omega)=2 \\ H_0(\omega+\pi)G_0(\omega)+H_1(\omega+\pi)G_1(\omega)=0 \end{cases} \tag{1}$$

In equation (1), H_0 and H_1 represent the decomposition filters in the horizontal and vertical directions respectively, G_0 and G_1 represent the synthesis filters in the two directions respectively, and H_1 represents the reconstruction angle. Then, the sampling matrix Q is used to rotate and down sample the target image. See equation (2) for details.

$$Q_0 = \begin{pmatrix} 1 & -1 \\ 1 & 1 \end{pmatrix}, \quad Q_1 = \begin{pmatrix} 1 & 1 \\ -1 & 1 \end{pmatrix} \tag{2}$$

In equation (2), Q_0 and Q_1 both represent the rotation and down sampling processing of the target image. The difference between them is that the rotation angles are 45° and -45° respectively. Signal clipping, also known as translation operation, is mainly to sort the image pixels twice in the process of decomposition and synthesis of the target image, and the processed image width is doubled.

2.2 Research on the basic structure of contour wave decomposition based on multi-core learning

Because CT is a double iterative filter bank, the LP and DFP contained in CT need to interact to complete the processing of the target image. Firstly, LP will decompose the target image, and then obtain the corresponding low-frequency subband and high-frequency subband. Then DFP will decompose the high-frequency band to obtain subbands in different directions, the number of which is 2^l, and the value range of l is any positive integer. Finally, the corresponding decomposition processing in different directions is repeated for the low-frequency subband (Jeevitha et al., 2019). Figure 2 shows the decomposition process of CT.

Figure 2 Decomposition diagram of CT

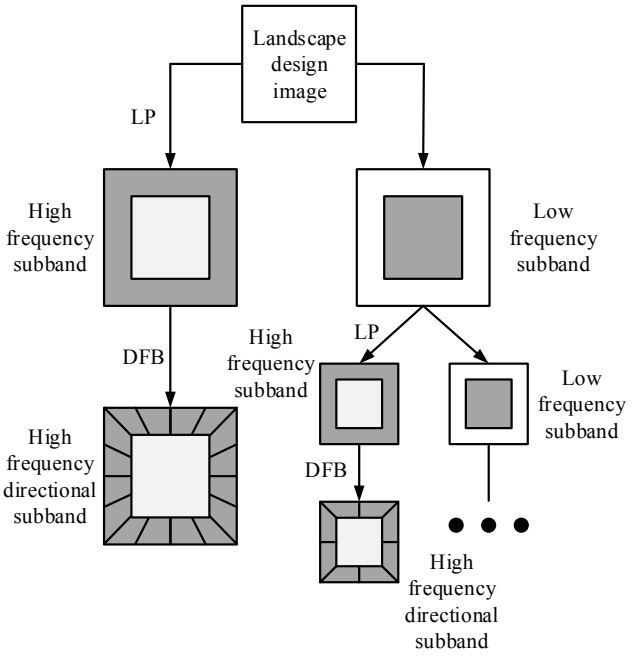

According to Figure 2, CT divides the processing of the target image into two parts, namely, low-frequency subband and high-frequency subband, mainly LP and DFP, so as to obtain subbands in different scales and directions. It should be noted that the number

of decomposition directions on any scale is 2^l, so as to ensure the multi-scale and multi-directional of target image processing. For the target image obtained after CT decomposition, certain measures need to be taken to ensure the image quality. Therefore, MKL can be used to accurately predict the image quality (Seethalakshmi and Valli, 2019; Zhang and Sun, 2019). Among the nuclear machine learning methods, MKL is a widely concerned learning method. Its main function is to improve the accuracy and effectiveness of image analysis in nonlinear mode. Traditional kernel machine learning methods mostly take a single kernel function as the core, such as support vector machine and extreme learning machine. It is difficult to ensure the accuracy of sample analysis when dealing with the problems of huge number of samples, disordered sample distribution, lack of regularity of heterogeneous data and so on. MKL can expand a large number of nuclear tissues, as shown in Figure 3.

Figure 3 Schematic diagram of nuclear organisation form of MKL

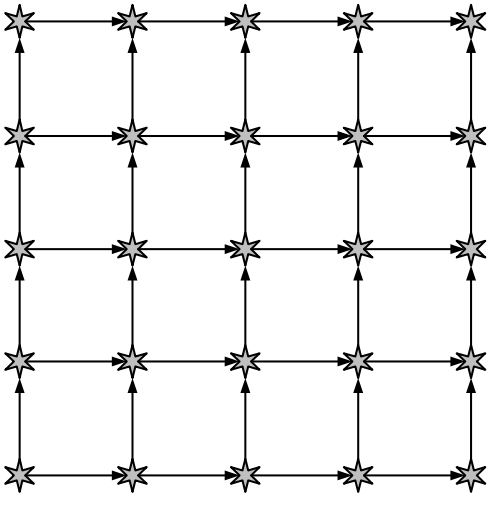

It can be seen from Figure 3 that MKL can effectively combine multiple kernel functions, abandon the disadvantage of taking a single kernel function as the main component, and achieve better image quality prediction effect by accurately, quickly and accurately classifying the feature matrix. MKL mainly integrates a large number of nuclear organisations to expand their combination into a more comprehensive directed acyclic graph, which represents different adjacency matrices under the action of sparsity, so as to realise the effective selection and optimisation of cores (Huang and Chen, 2020; Wang et al., 2019). MKL divides the input space to obtain several subspaces, and the reconstructed signal x can be expressed as equation (3).

$$x = x_1 \times x_2 \times \cdots \times x_p \tag{3}$$

In equation (3), p represents the number of subspaces, and p is determined as the sequence number of kernels. If the length of the core is expressed as $q+1$, the core of MKL is shown in formula (4).

$$k(x,x') = \prod_{i=1}^{p}\left(\sum_{j_i=0}^{q} kij_i(x_i,x_i')\right) \tag{4}$$

The number of base nuclei that can be obtained according to formula (4) is $(q+1)^p$. When selecting a large number of nonlinear variables, MKL has significant advantages, especially polynomial kernel and Gaussian kernel (Zhang and Nie, 2019). The overall density curve of MKL can be regarded as the overall combination of multiple polynomial curves, so the whole polynomial kernel can be expressed as equation (5).

$$k(x,x_t') = \prod_{i=1}^{p}(1+x_i x_t')^q = \sum_{j_i,\cdots,j_p=0}^{q}\sum_{i=1}^{p}\binom{q}{j_i}(x_i,x_t')^{j_i} \tag{5}$$

In equation (5), $k(x,x_t)$ represents a kernel function composed of multiple kernels.

2.3 Research on image noise elimination based on contour wave transform

In the process of image feature extraction, noise reduction or denoising should be carried out first. The denoising method based on contour wave transform is mainly threshold shrinkage denoising. For the target image with a lot of noise, the threshold shrinkage denoising method first processes the correlation coefficient after contour wave decomposition. Then, judge the value of the coefficient. If its amplitude is less than the established threshold, it is necessary to take corresponding measures to set the coefficient to zero or shrink. Finally, through the function of inverse transformation, the target of eliminating noise in the target image is realised (Li et al., 2020; Fang, 2019). The traditional global threshold denoising method has certain application results, but this method cannot deal with and solve the problem of differences in decomposition coefficients of different layers. Therefore, on this basis, the threshold denoising method, multi-scale layered threshold, is optimised. See equation (6) for details.

$$\delta_j = \sigma\sqrt{2\ln(N)}\times 2^{(j-J)/2} \quad (j=0,\ldots,J-1) \tag{6}$$

In equation (6), N represents the total number of pixels of the target image. J and j represent the decomposition scale and grade respectively. σ represents the standard deviation of noise, and its expression can be expressed by median method, as shown in equation (7).

$$\sigma = median(|C_1|)/0.6745 \tag{7}$$

In equation (7), C_1 represents the contour wave coefficient set at the corresponding decomposition scale. In order to further optimise and improve the multi-scale layered threshold method and improve its denoising effect, this study combines the size of subband energy in different directions of contour wave and the action relationship between different contour details, and takes this as the basis to correct the original threshold, and finally achieve the purpose of noise elimination (Fang et al., 2020; Gong et al., 2020). In the high-frequency direction subband after contour wave

decomposition, the subband containing large energy can be used as the representative of the obvious features of the image, so equation (8) can be obtained.

$$E_j^l = \sum_x \sum_y \left[f_j^l(x,y) \right]^2 \quad (j = 1,2,3,\ldots \ \ l = 1,2,3,\ldots) \tag{8}$$

In equation (8), E_j^l represents the high-frequency subband energy from the *l*th direction of layer *j* after contour wave decomposition; $f_j^l(x,y)$ represents the high-frequency subband coefficient at the same position. Accordingly, the high-frequency subband energy can be processed to obtain the corresponding average energy $\overline{E}$, as shown in equation (9).

$$\overline{E} = \left(E_j^1 + E_j^2 + E_j^3 + \cdots + E_j^l \right) / l \quad (l = 1,2,3,\cdots) \tag{9}$$

Under the action of multi-level decomposition, the target image with noise will show different energy distribution. When the image is located at the same scale but in different subband directions, the size of energy value plays a key role in the number of contour details, and the two are positively correlated (Zhao et al., 2019). Based on this, if the threshold is set low, more image contour features can be retained as much as possible; If the set threshold is expanded, the elimination of image noise can be maximised. Through the threshold correction coefficient λ, the threshold δ_j of the contour wave multi-scale decomposition threshold method can be modified to a certain extent. Equation (10) shows the calculation expression of λ.

$$\lambda = \overline{E} / E_j^l \tag{10}$$

The corrected image threshold ξ_j can be obtained according to equation (10), as shown in equation (11).

$$\xi_j = \lambda \delta_j \tag{11}$$

3 Effect analysis of texture feature extraction of landscape design image based on contour wave transform

3.1 Image feature extraction results based on contour wave transform

In order to explore the effect of texture feature extraction of landscape design image based on contour wave transform, this study selects the public database live as the main research object. The live database mainly contains five types of distorted images. 500 images in the real-time database are selected as the experimental dataset, mainly white noise pollution, rapid degradation and Gaussian blur. Different types of images have corresponding subjective scores (DMOS). The value range of DMOS is [1,100], and its size is negatively correlated with the image quality. After applying the denoising method of contour wave transform, there will be some differences in the extraction of image features and the evaluation of image quality. This topic will use the linear correlation coefficient (LCC) and Spearman Rank Order Correlation Coefficient (SROCC) are used as evaluation indicators. The closer the value of LCC to 1, the better the feature extraction effect of this method and the higher the image quality; the value range of

SROCC is [–1,1], the closer the value is to the boundary value, the higher the monotonicity of the image quality evaluation method. Random sampling experiments were conducted on live database, and the LCC score results obtained are shown in Figure 4.

Figure 4 LCC scoring results of LIVE database

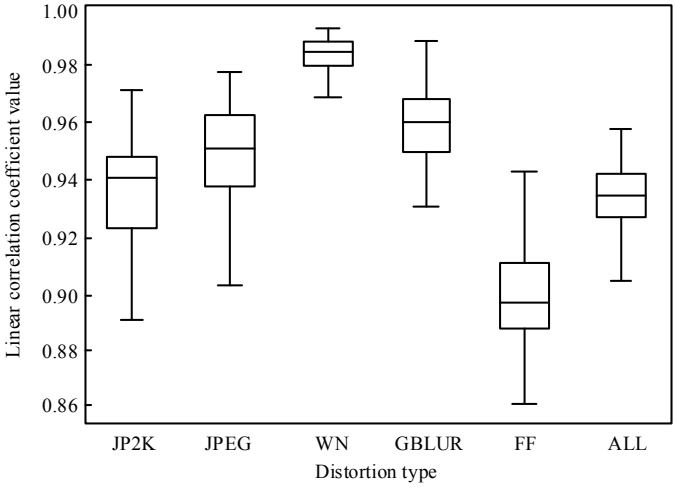

Figure 4 shows that in addition to rapid degradation, in other types of distorted images such as white noise pollution and Gaussian blur, the algorithms proposed in this study have good stability, and the difference between the corresponding LCC values is small. Then, for stock, live database is used for analysis, and the results are shown in Figure 5.

Figure 5 SROCC scoring results of LIVE database

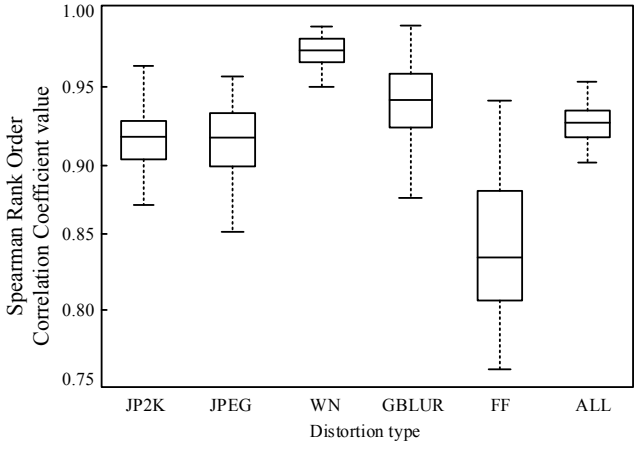

Compared with LCC scoring results, the difference of SROCC scoring results is more significant, and the difference between images classified as rapid degradation in the database and other types of images is greater. The main reason for this phenomenon is

that rapid degradation is a multi-process image distortion phenomenon, which will cause diversified distortion effects on the image itself, its feature extraction and quality evaluation, and finally make the detection and extraction of this kind of image distortion phenomenon significantly more difficult than other image distortion types. On the whole, the image feature extraction and quality evaluation based on contour wave transform has good application effect. When mixing all image distortion types, it can also obtain better extraction and evaluation results. In order to further verify the effectiveness of the method proposed in this study, compare it with the Blind Image Quality Assessment (BIQA) algorithm, Natural Scene Statistics (NSS) and Blind / Referential Image Spatial Quality Evaluator (BRISQUE) algorithm, and obtain the SROCC comparison results shown in Table 1.

Table 1 SROCC comparison results of different algorithms in LIVE mixed distortion image database

Algorithm	*Blind/FR*	*BLUE & JPEG*	*BLUE & WN*	*OVERALL*
Paper algorithm	Blind	0.9066	0.8822	0.9030
BRISQUE	Blind	0.7915	0.2129	0.4221
NSS	Blind	0.8926	0.8972	0.9010
BIQA	FR	0.8340	0.8549	0.8444
VIF	FR	0.8785	0.8739	0.8864
VSNR	FR	0.7751	0.7565	0.7834
PSNR	FR	0.6624	0.7067	0.6944

As can be seen from Table 1, Compared with other algorithms mentioned above, the algorithm proposed in this study has more significant advantages in the mixed distortion image database, which is mainly reflected in the accurate image quality evaluation for different types of distorted images, and the image features extracted from the target image, can reflect their own distortion changes completely and efficiently. Arbitrarily select a landscape design image from the LIVE database and compare the image feature extraction of different algorithms. See Figure 6 for details.

Figure 6 Comparison of image feature extraction accuracy and extraction speed of different algorithms

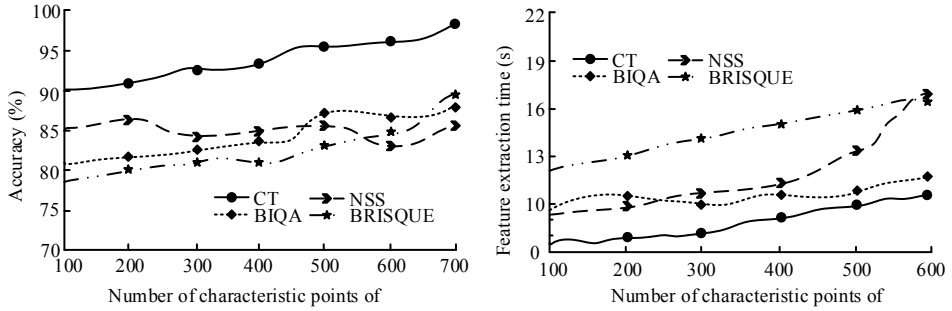

(a)Comparison of image texture feature extraction accuracy of different algorithms

(b)Comparison of image texture feature extraction speed with different algorithms

Figure 6(a) shows that with the increasing number of degraded distortion trend feature points, the image feature extraction accuracy of different algorithms shows a certain increase, especially the feature extraction algorithm based on contour wave transform. When the number of degraded distortion trend feature points is only 100, the extraction accuracy of the feature extraction algorithm based on contour wave transform has been at the level of 90%, and has maintained a continuous upward trend, which is always significantly higher than the image texture feature extraction accuracy of other algorithms. Figure 6(b) shows the comparison results of image texture feature extraction speed of different algorithms. The feature extraction time of all algorithms will continue to extend with the increase of the number of feature points. The feature extraction algorithm based on contour wave transform always keeps the minimum time, and its average level is about 5S, which is significantly lower than that of other algorithms, indicating that the extraction speed of the algorithm is the best and can effectively extract the texture features of the target image.

3.2 Comparison of robustness of image texture feature extraction under different conditions

In order to analyse the robustness of the texture feature extraction algorithm of landscape design image based on contour wave transform, this study adopts different processing methods for the target image, including changing the light intensity, strengthening the influence of noise, compressing the image quality and so on, in order to obtain the robustness under different conditions. Firstly, a certain number of target images are randomly selected from the live database, which are respectively set as training image set and test image set according to the ratio of 7 : 3, and tested for 50 times. The test results of feature extraction robustness under different brightness conditions are shown in Table 2.

Table 2 Robustness of image texture feature extraction algorithm under different brightness conditions

Brightness enhancement	*Recall* (%)	*Precision rate* (%)	*Accuracy* (%)
Original image	96.24	94.45	95.42
10%	96.31	96.31	96.34
30%	94.45	94.45	94.51
50%	94.45	91.08	92.67
–10%	92.60	90.92	91.75
–30%	90.75	90.75	90.84

According to Table 2, when the brightness of the environment where the target image is located is enhanced by 10%, the accuracy of image texture feature extraction shows a slight upward trend, because the texture features of the target image will be more clearly visible under the condition of brightness enhancement; When the brightness continues to increase by 30% and 50%, the accuracy is close to the original image accuracy and decreases, but still remains above 90%. When the brightness is negatively increased, the accuracy will be significantly reduced, but still above the 90% level. This shows that too bright or too dark lighting environment will increase the difficulty of image texture

feature extraction, and reduce the accuracy of feature extraction algorithm to a certain extent. Nevertheless, the texture feature extraction algorithm of landscape design image based on contour wave transform is still robust to different brightness conditions. The robustness results under different noise effects are shown in Figure 7.

Figure 7 Robustness of image feature extraction algorithm under different degrees of noise

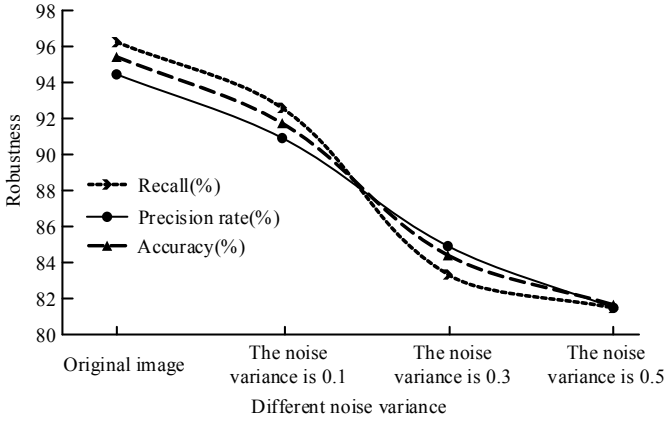

According to Table 2, when the brightness of the environment where the target image is located is enhanced by 10%, the accuracy of image texture feature extraction shows a slight upward trend, because the texture features of the target image will be more clearly visible under the condition of brightness enhancement. When the brightness continues to increase by 30% and 50%, the accuracy is close to the original image accuracy and decreases, but still remains above 90%. When the brightness is negatively increased, the accuracy will be significantly reduced, but still above the 90% level. This shows that too bright or too dark lighting environment will increase the difficulty of image texture feature extraction, and reduce the accuracy of feature extraction algorithm to a certain extent. Nevertheless, the texture feature extraction algorithm of landscape design image based on contour wave transform is still robust to different brightness conditions. The robustness results under different noise effects are shown in Figure 7.

It can be seen from Figure 8 that different degrees of quality compression processing on the image will have a great impact on its accuracy and other indicators. When the compression mass is 90%, the decrease of accuracy is small, from 95.42% to 94.50%. When the compression quality is 70%, the recall, precision and accuracy of the texture feature extraction algorithm of landscape design image based on contour wave transform are reduced to less than 90%. When the compression quality is 50%, the accuracy of the proposed algorithm is reduced to 73.40%. This shows that with the reduction of compression quality, the accuracy of the algorithm will also decrease, and the change trend is obvious. The main reason is that this method uses multi-core learning (MKL) to accurately predict the image quality, combined with the sub-band energy of contour waves in different directions and the action relationship between different contour details, based on which the original threshold is corrected, and finally achieve the purpose of denoising.

Figure 8 Robustness of image feature extraction algorithm under different quality compression conditions

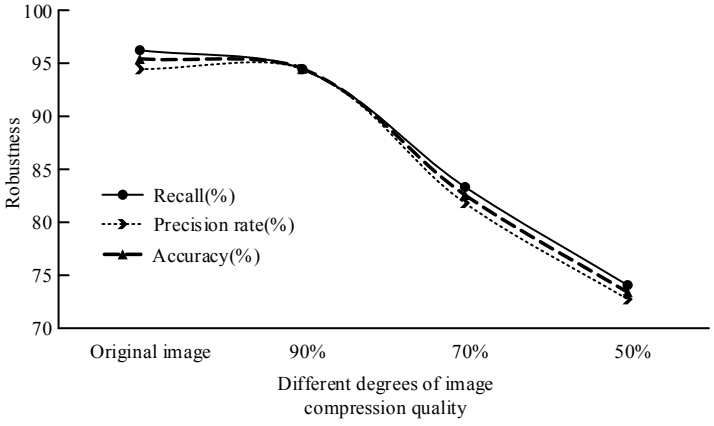

4 Conclusion

With the continuous development of social economy and computer technology, image processing technology has made great progress, and the extraction of image texture features has attracted much attention. In order to ensure the effectiveness and safety of landscape design image texture feature extraction, this study takes contour wave transform as the main research object, and explores its application effect in landscape design image texture feature extraction through its structure, action mechanism and denoising processing method. Through the analysis of relevant simulation experiments, it is verified that the algorithm has the significant advantages of high image feature extraction accuracy, short feature extraction time and strong robustness. Under different interference conditions, the robustness of the texture feature extraction algorithm of landscape design image based on contour wave transform is different. For the feature extraction of the original image, the recall, precision and accuracy are as high as 96.24%, 94.45% and 95.42% respectively. This shows that the application effect of texture feature extraction of landscape design image based on contour wave transform is superior, and can provide reliable data support for the optimal design of landscape. Although this study is lucky to have achieved some results, there are few gradients in the comparative experiment, and we hope to improve them in the future.

References

Ch, M., Riaz, M.M., Iltaf, N., Ghafoor, A. and Ahmad, A. (2019) 'Weighted image fusion using cross bilateral filter and non-subsampled contourlet transform', *Multidimensional Systems and Signal Processing*, Vol. 30, No. 3, pp.2199–2210.

El-Hoseny, H.M., El-Rahman, W.A., El-Shafai, W., El-Rabaie, E.M., Mahmoud, K.R., El-Samie, F.A. and Faragallah, O.S. (2019) 'Optimal multi-scale geometric fusion based on non-subsampled contourlet transform and modified central force optimization', *International Journal of Imaging Systems and Technology*, Vol. 29, No. 1, pp.4–18.

Fang, L. (2019) 'An image segmentation technique using nonsubsampled contourlet transform and active contours', *Soft Computing*, Vol. 23, No. 7, pp.1823–1832.

Fang, L., Zhang, H., Zhou, J. and Wang, X.H. (2020) 'Image classification with an RGB-channel nonsubsampled contourlet transform and a convolutional neural network', *Neurocomputing*, Vol. 396, pp.266–277.

Gong, L.H., Tian, C., Zou, W.P. and Zhou, N.R. (2020) 'Robust and imperceptible watermarking scheme based on canny edge detection and SVD in the contourlet domain', *Multimedia Tools and Applications*, Vol. 2020, No. 4, pp.439–461.

He, G., Xing, S., He, X., Wang, J. and Fan, J.P. (2019) 'Image fusion method based on simultaneous sparse representation with non-subsampled contourlet transform', *IET Computer Vision*, Vol. 13, No. 2, pp.240–248.

Huang, Y.H. and Chen, D.W. (2020) 'Image fuzzy enhancement algorithm based on contourlet transform domain', *Multimedia Tools and Applications*, Vol. 79, No. 4, pp.35017–35032.

Jeevitha, S. and Amutha Prabha, N. (2019) 'Effective payload and improved security using HMT contourlet transform in medical image steganography', *Health and Technology*, Vol. 1, No. 10, pp.217–229.

Li, J.Y. and Zhang, C.Z. (2020) 'Blind watermarking scheme based on Schur decomposition and non-subsampled contourlet transform', *Multimedia Tools and Applications*, Vol. 79, No. 12, pp.30007–30021.

Li, X., Liu, Z., Yin, G. and Jiang, H. (2020) 'Ferrite magnetic tile defects detection based on nonsubsampled contourlet transform and texture feature measurement', *Russian Journal of Nondestructive Testing*, Vol. 56, No. 4, pp.386–395.

Liu, H., Xiao, G.F., Tan, Y.L. and Ouyang, C.J. (2019) 'Multi-source remote sensing image registration based on contourlet transform and multiple feature fusion', *International Journal of Automation and Computing*, Vol. 16, No. 05, pp.15–28.

Liu, X., Xu, K., Zhou, D. and Zhou, P. (2019) 'Improved contourlet transform construction and its application to surface defect recognition of metals', *Multidimensional Systems and Signal Processing*, Vol. 31, No. 11, pp.951–964.

Seethalakshmi, K. and Valli, S. (2019) 'A fuzzy approach to recognize face using contourlet transform', *International Journal of Fuzzy Systems*, Vol. 21, No. 201, pp.2204–2211.

Subhedar, M.S. and Mankar, V.H. (2019) 'Image steganography using contourlet transform and matrix decomposition techniques', *Multimedia Tools and Applications*, Vol. 78, No. 15, pp.22155–22181.

Vaidya, S.P. (2019) 'A blind color image watermarking using BRISK features and contourlet transform', *RTIP2R 2018: Recent Trends in Image Processing and Pattern Recognition*, Vol. 7, No. 2019, pp.203–215.

Wang, X.Y., Zhang, S.Y., Wen, T.T., Yang, H.Y. and Niu, P.P. (2019) 'Coefficient difference based watermark detector in nonsubsampled contourlet transform domain', *Information Sciences*, Vol. 503, pp.274–290.

Zhang, C.J. and Nie, H.H. (2019) 'An adaptive enhancement method for breast X-ray images based on the nonsubsampled contourlet transform domain and whale optimization algorithm', *Medical and Biological Engineering and Computing*, Vol. 57, No. 2, pp.2245–2263.

Zhang, Y. and Sun, Y. (2019) 'An image watermarking method based on visual saliency and contourlet transform', *Optik – International Journal for Light and Electron Optics*, Vol. 186, pp.379–389.

Zhao, B., Ren, Y., Gao, D., Xu, L.Z. and Zhang, Y.Y. (2019) 'Thermo dynamic methodology of A type microreactor based on contourlet finite element method', *International Journal of Hydrogen Energy*, Vol. 44, No. 33, pp.18586–18596.

Zhu, D.D., Wang, B., Yang, Y. and Li, Y.B. (2019) 'Asphalt infrared image enhancement of combining contourlet transform with genetic algorithm', *Jiliang Xuebao/Acta Metrologica Sinica*, Vol. 40, No. 1, pp.25–30.